Surface Science 603 (2009) 304–310

Contents lists available at ScienceDirect

Surface Science

journal homepage: www.elsevier.com/locate/susc

Density functional and dynamics study of the dissociative adsorption of hydrogen on Mg (0001) surface

D. Kecik, M.K. Aydinol *

Department of Metallurgical and Materials Engineering, Middle East Technical University, 06531 Ankara, Turkey

ARTICLE INFO

Article history:
Received 8 July 2008
Accepted for publication 17 November 2008
Available online 30 November 2008

Keywords:
Density functional calculations
Molecular dynamics
Magnesium hydride
Hydrogen adsorption

ABSTRACT

A first principles study is performed to investigate the adsorption characteristics of hydrogen on magnesium surface. Substitutional and on-surface adsorption energies are calculated for Mg (0001) surface alloyed with the selected elements. To further analyze the hydrogen–magnesium interaction, first principles molecular dynamics method is used which simulates the behavior of H_2 at the surface. Also, charge density differences of substitutionally doped surface configurations were illustrated. Accordingly, Mo and Ni are among the elements yielding lower adsorption energies, which are found to be −9.2626 and −5.2995 eV for substitutionally alloyed surfaces, respectively. In light of the dynamic calculations, Co as an alloying element is found to have a splitting effect on H_2 in 50 fs, where the first hydrogen atom is taken inside the Mg substrate right after the decomposition and the other after 1300 fs. An interesting remark is that, elements which acquire higher chances of adsorption are also seen to be competent at dissociating the hydrogen molecule. Furthermore, charge density distributions support the results of molecular dynamics simulations, by verifying the distinguished effects of most of the 3*d* and 4*d* transition metals.

1. Introduction

The fact that fossil fuel reserves are expected to diminish in the near future and cause serious environmental pollution highlights the significance of hydrogen, as being an abundant, environmentally benign and efficient energy carrier. The reversible storage of hydrogen for both stationary and mobile applications can be in several forms, such as gaseous, liquid, carbon nanotubes, metal and complex hydrides [1]. Besides the advantage of metals being highly reactive with hydrogen, in the hydride form they are capable of storing hydrogen in large amounts on a reversible basis [2]. The generally searched criteria for an ideal metal hydride are high storage capacity, fast hydrogenation/dehydrogenation kinetics, low desorption temperatures as well as low cost. Magnesium hydride (MgH_2), in this respect is a promising material being economic, light weight and storing high amounts of hydrogen (7.6 wt.%), despite its high reactivity towards air and oxygen and high thermodynamical stability, which leads to poor hydriding/dehydriding kinetics [3]. In order to decrease the hydrogen desorption temperature which is above 300 °C, there are several methods such as altering the chemical composition, mechanical alloying and addition of catalysts. Zaluska et al. [4] pointed out two major reasons for poor dehydrogenation kinetics as, oxide layer formation and slow dissociation rate of hydrogen on magnesium surface. It was also mentioned that since the MgO layer impedes hydrogen penetration inside the surface, the oxide layer needs to be cracked by annealing at a temperature above 400 °C, so that the metal surface would be exposed to hydrogen. Furthermore, in their study, the conclusion has been raised that small amounts of catalysts (like Pd or Fe) would induce the improvement of hydrogenation kinetics. Besides palladium, Baer et al. [5] claimed that nickel is also an outstanding catalyst since it holds the ability to dissociate and adsorb the hydrogen molecule. Titanium and vanadium, as stated by Liang et al. [6] are as well favored catalysts for hydrogen absorption. Although their strong tendency towards oxidization makes the catalytic effect disappear. Moreover, addition of oxide catalysts, such as Cr_2O_3, V_2O_5 and Fe_3O_4 [7], were found useful in achieving improved hydriding properties at lower temperatures. Dornheim et al. [8], have stressed the effect of 3*d* transition metals in their study, in terms of the reduction of hydride formation enthalpies. Nevertheless, alloying with 3*d* elements was seen to give rise to a decline in the hydrogen storage capacity below 3.6 wt.%.

Sprunger and Plummer [9], on the other hand, executed a study based on the comparison of experimental and theoretical results. Regarding the interaction of H_2 with Mg (0001) surface, the tools used were electron energy loss spectroscopy (EELS), thermal desorption spectrometry (TDS), core level spectroscopy and work-function measurements. In their study, as a result of the

* Corresponding author. Tel.: +90 312 210 2523; fax: +90 312 210 2518.
E-mail address: kadri@metu.edu.tr (M.K. Aydinol).

0039-6028/$ - see front matter © 2008 Elsevier B.V. All rights reserved.
doi:10.1016/j.susc.2008.11.017

exposure of pure Mg (0001) surface (≥110 K) to hydrogen at room temperature, not only it was unlikely to observe molecular adsorption of H_2, but also dissociative chemisorption did not take place under the temperature conditions in question. This result is supported with the outcome of theoretical calculations, which stress the high activation barrier for H/simple metal systems. Bird et al. [10] indicated that, as a result of the interaction between hydrogen and metal surface, the non-bonding orbital of the metal is being filled. Moreover, their study revealed that with a barrier of 0.4 eV, the adsorption site preferred by H_2 is the bridge site between the two metal atoms. Furthermore, Ravindran et al. [11] have studied complex hydrides, making use of charge density, charge transfer, electron localization function, partial densities of states, Mulliken population analysis and Born effective charges. Finally, they have reached the conclusion that, due to their weaker bonding characteristics, the interstitial sites are favored by hydrogen in metals, alloys and intermetallic structures. Vegge [12] in his study, where he made use of the nudged elastic band method (NEB), presented the rate-limiting step for adsorption of hydrogen on Mg (0001) surface as the dissociation, whereas that for desorption was concluded to be the rejoining of H_2. The potential energy surface (PES) results for hydrogen action on magnesium put forward the rate-limiting character of dissociation step by yielding large activation energies for this and diffusion of dissociated hydrogen into the first layer of Mg slab. In another study of Vegge and his co-workers [13], it was deduced that 3*d* transition metals would be beneficial in improving both the adsorption and desorption kinetics for MgH_2, in case magnesium is properly alloyed with 3*d* transition elements. In addition, Pozzo et al. [14] detected the improvement of H_2 intake kinetics through Mg surface, via doping Ni and Ti as the adsorbates, where the interaction of their unfilled *d* orbitals and *s* electron of hydrogen is seen to be predominant over Mg–H bonding.

Apart from the studies on hydrogen interaction with magnesium surface, Kiejna et al. [15], have examined the adsorption of low-coverage alkali adatoms on (0001) surface of Mg. The results show that, potassium would prefer hollow sites, where its relatively large size disables the adsorption on substitutional sites.

In this study, we aimed to investigate the manners for hydrogen dissociation and adsorption on Mg surface and suggest a systematic trend within the periodic table in terms of the catalyzer effects of selected elements. Correspondingly, substitutional and on-surface adsorption energies regarding Mg (0001) surfaces doped with one adatom were computed via the ab-initio total energy pseudopotential methods. In addition, first principles molecular dynamics calculations were performed for structures also including the hydrogen molecule. Finally, charge density difference distributions were illustrated for substitutionally alloyed Mg surface systems.

2. Computational method

All computations in this study have been performed using plane-wave pseudopotential where fully self-consistent density functional theory (DFT) calculations were used to solve Kohn-Sham equations. Ab-initio total energy and molecular dynamics calculations were executed using the VASP (Vienna ab-initio simulation package) code developed at the Institut fur Materialphysik of the Universitat Wien [16–18]. The generalized gradient approximation (GGA) implementation by Perdew et al. [19] was exploited where the core electrons were replaced by Vanderbilt ultrasoft pseudopotentials (US-PP) [20].

For surface calculations of magnesium, a slab consisting of $3 \times 3 \times 1$ unit cells (six atomic layers) of Mg was created. The positions of atoms in surface structure of magnesium were set according to the relaxed coordinates in bulk Mg. One atomic layer at the bottom was fixed during the calculations. A vacuum range of up to 20 Å has been used in modeling the surface and approximately after 11 Å, no appreciable difference was seen in the top layer atomic coordinates after relaxation. During the relaxation calculations of alloyed surface systems, we have initially used the relaxed coordinates of pure Mg surface. Furthermore, we have calculated the percent change in coordinates of atoms located just above the fixed bottom layer, for pure Mg and Co doped surfaces due to relaxation. They are 4.5% and 0.14%, respectively, from which slab thickness chosen was decided to be adequate.

We first aimed to investigate the substitutional adsorption behavior of selected alloying elements on (0001) surface of Mg. There are 53 Mg atoms and one M atom (substituted in place of a magnesium atom at the center of the uppermost layer, creating a concentration of 0.93 at.%) in the slab. Within the alloying elements studied, there are 3*d* transition metals (the entire row), 4*d* transition metals from Zr to Mo and Pd to In, some heavy metals such as Au and Pb, some alkaline elements and also some nonmetals like P and Ge. For the purpose of obtaining the lowest energy configuration, systems were allowed to relax in terms of all atomic degrees of freedom, while the cell size and shape were kept constant. *k*-point implementation was performed on the gamma point only. The differences in the substitutional adsorption energy for some of the elements studied between gamma point only and $2 \times 2 \times 1$ *k*-point mesh calculation were found to be less than 19 meV per cell. Additional spin polarized calculations performed for Fe, Ni and Co doped systems were not seen to create a significant effect energetically, with respect to the non-spin polarized calculations.

Adsorption energy for substitutionally doped Mg (0001) surface structures (represented by $E_{\text{sub-ads,Mg(0001)}}$) is calculated via the following equation [21]:

$$E_{\text{sub-ads,Mg(0001)}} = E_{\text{M/Mg(0001)}} - E_{\text{Mg(0001)}} - E_{\text{M-atom}} + E_{\text{Mg-step}} \quad (1)$$

where $E_{\text{M/Mg(0001)}}$ and $E_{\text{Mg(0001)}}$ represent the total energies of substitutionally alloyed and pure magnesium surface structures, respectively. $E_{\text{M-atom}}$ represents the energy of the adatom, which was put as a single atom in a box of $10 \times 10 \times 10$ Å, calculated with single *k*-point. Besides, $E_{\text{Mg-step}}$ stands for the energy of Mg atom (to be substituted by M atom) which is considered to be removed from the top plane and brought to a step or kink site at the surface. For the calculation of this term, one magnesium atom was located on the surface at a regular lattice point as if the surface extends towards vacuum. Next, the difference between total energies calculated for this configuration and normal Mg surface without this extension was taken, which yields the term $E_{\text{Mg-step}}$.

For all relaxation calculations, 10^{-3} eV energy difference was set as the convergence criterion between successive ionic steps. We have also determined the dipole corrections to the total energy. It was found to be less than 1 meV per cell, which was then neglected in all calculations.

We then studied on-surface (normal) adsorption. Adatoms were placed slightly above the surface (1.6–1.8 Å) which were then relaxed, in three different positions, which are hollow, top and bridge, as illustrated in Fig. 1, produced by VESTA [22]. Calculation of on-surface adsorption energies for normally doped Mg (0001) surface (expressed as $E_{\text{nor-ads,Mg(0001)}}$) is via the equation shown as follows [21]:

$$E_{\text{nor-ads,Mg(0001)}} = E_{\text{M/Mg(0001)}} - E_{\text{Mg(0001)}} - E_{\text{M-atom}} \quad (2)$$

where $E_{\text{M/Mg(0001)}}$ and $E_{\text{Mg(0001)}}$ represent the total energies of normally doped and pure Mg surfaces, respectively. Here again, $E_{\text{M-atom}}$ is the energy of the adsorbed species. In addition, the vibrational frequencies for the alloying elements adsorbed on-surface were also calculated to elucidate the nature of each site.

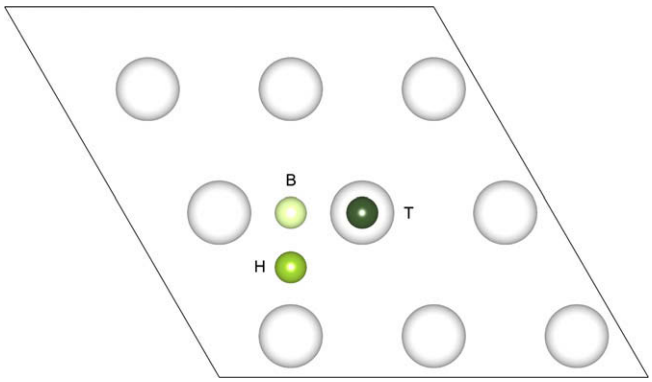

Fig. 1. Top view of Mg (0001) surface structure. Large circles denote magnesium atoms, small circles represent the adatom where the lightest in color stands for the adatom doped at bridge adsorption sites, relatively darker one for hollow and the darkest for top sites.

For the next part of the study, we performed first principles molecular dynamics (MD) calculations with the motivation of determining hydrogen adsorption characteristics on Mg (0001) surface. Here again, a box (where the atomic positions are initially set as were found in the relaxed bulk structure of Mg) with a slab size of $3 \times 3 \times 1$, with 53 Mg atoms and one M atom and a vacuum range of approximately 11 Å at the top was created. *k*-point implementation was performed on gamma point only. Moreover, surface temperature controlled by a Nosé thermostat [23,24] and time step per each ionic motion were specified as 300 K and 0.2 fs, respectively. The hydrogen molecule, oriented parallel and vertical to the surface, was positioned in the vacuum at different heights above the surface, such as 1, 1.5 and 2 Å. Subsequently, a distance of 1.5 Å to the uppermost layer was seen to be sufficient in order to initiate an interaction between the hydrogen and surface atoms. It was observed that the vertically oriented molecule immediately rotates and becomes parallel. In all calculations then, parallel orientation was used as the starting configuration. Fig. 2 displays the initial orientation set for H_2, which is near the top of an atomic position occupied by an alloying element. Upper five layers of Mg atoms were allowed to relax while the very bottom layer was kept fixed.

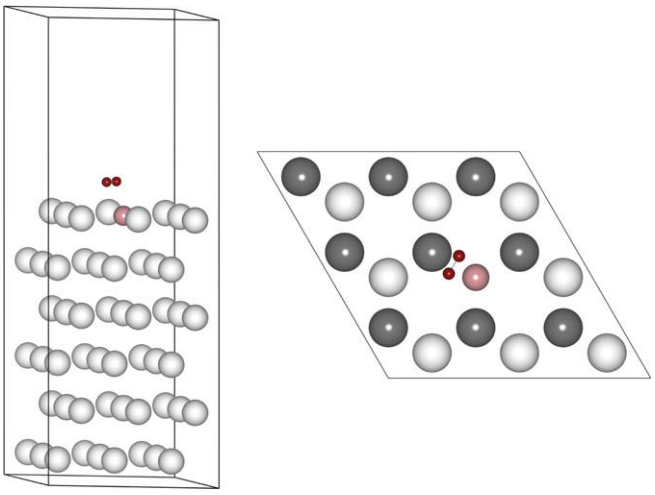

Fig. 2. Molecular dynamics cell of (0001) surface of Mg, from front and top views. In the top view, light colored large circles represent the uppermost Mg atoms at the surface (smaller is the adatom), while the sub-layer Mg atoms are indicated by dark color.

Furthermore, charge density difference distributions over surfaces of substitutionally alloyed magnesium were illustrated in order to describe the interaction of adatoms and surrounding ones, so that the reason behind H_2 dissociation could be elucidated to some extent.

3. Results and discussion

The calculations made in the bulk state predict the crystal properties of Mg in very close agreement with the experimental values. Experimental lattice constants *a* and *c* for hexagonal Mg are 3.213 and 5.213 Å [25], where theoretically calculated values were found to be 3.190 and 5.192 Å, respectively. In this regard, percent errors in calculation of the equilibrium lattice parameters *a* and *c*, relative to the experimental values were achieved as ~0.7% and 0.4%. Moreover, formation energy of magnesium hydride, MgH_2, has been calculated in kJ on the basis of one mole of hydrogen molecule, which was obtained as −72.016 kJ/mol-H_2. This is very close to the experimentally measured value by Bogdanovic et al. [26] which is −73.5 kJ/mol-H_2. Another supporting result was proposed by Song et al. [27], where they have calculated ΔE_f of MgH_2 as −71.15 kJ/mol-H_2.

3.1. Surface-substitutional adsorption

As may be recalled, for surface alloying studies of Mg (0001) structure, selected elements were doped in four different positions. The first site is where an alloying element substitutes for a magnesium atom in the center of the uppermost layer, and is referred to as substitutional adsorption. The calculation of the adsorption energy for these systems was explained previously. Adsorption energy values of substitutionally alloyed Mg (0001) surface, represented by $E_{\text{sub-ads,Mg(0001)}}$, are tabulated in Table 1 for each system. The results show that all of these thirty two elements would be adsorbed on Mg surface (in terms of their negative adsorption energies). Furthermore, elements acquiring the potential of being adsorbed on substrate Mg more extensively with respect to the others are Mo, Nb, Cr, Mn, Fe, V, Zr, Hf, Co, P, Ti and Ni, respectively. Surface-substitutional adsorption energies of the mentioned species vary between −9.2626 (Mo) and −5.2995 eV (Ni). On the other hand, the highest energy value is that of Cd within all elements, which was found as −0.5628 eV. Besides, an interesting remark attained from the ionic relaxations performed on these substitutionally alloyed Mg (0001) surfaces is the correlation between final configurations and adsorption energies. More specifically, it was observed that, elements within systems holding lower adsorption energies tend to be attracted inside the lattice, whereas dopants present in systems having higher energies (thus lower chance of adsorption) are elevated in the vacuum region to an extent. Within the stated elements that yield lowest adsorption energies for substitutionally alloyed Mg surfaces, Mo, Nb, Cr, Mn, Fe, V, Co, P, Ti and Ni are among the ones which also are attracted inside the vacuum considerably. The extents they have descended below the surface (relative to the initial position of the top layer) could quantitatively be expressed as, 0.989, 0.655, 0.564, 0.551, 0.538, 0.535, 0.527, 0.521 and 0.510 Å for the adatoms P, Ni, V, Cr, Nb, Ti, Co, Mo and Mn, respectively. On the other hand, Cd, K and Na are examples to the dopants which give rise to higher adsorption energies and are elevated above the surface at the same time. The amount of elevation from the surface was observed to be 2.265, 1.310 and 0.381 Å for the substitutional elements K, Na and Cd, respectively.

Alongside these observations, a general trend has been realized related to the behavior of substitutionally placed dopants after surface relaxations. That is, for systems with adsorption energies

Table 1
Substitutional and on-surface adsorption energy values (in eV) and MD results for alloyed Mg surface. "S" represents splitting of H_2 by the dopant and "NS" the non-splitting of hydrogen atoms. "E" denotes early attraction of hydrogen into the lattice, while "L" late intake of H atom under the surface, by the splitting elements. Additional to the MD results tabulated, catalyzer effect of **Ru (S, L)** and **Rh (S, L)** elements has also been observed.

Dopant	$E_{sub\text{-}ads,Mg(0001)}$	$E_{nor\text{-}ads,Mg(0001)}$	MD
Pure	–	–	NS
Li	−1.4426	−1.7091 (B)	NS
Na	−0.9249	−1.2978 (H)	NS
Al	−2.8573	−2.8290 (B)	NS
Si	−4.8953	−4.6039 (B)	NS
P	−6.1820	−6.2662 (B)	NS
K	−0.7052	−1.3025 (B)	NS
Ca	−1.6708	−1.3743 (H)	NS
Sc	−4.4122	−2.7642 (H)	NS
Ti	−5.7472	−3.7261 (T)	**S, L**
V	−6.8671	−6.2998 (H)	**S, L**
Cr	−7.5106	−7.4238 (H)	**S, E**
Mn	−7.5063	−7.7339 (B)	**S, E**
Fe	−7.0414	−7.3799 (B)	**S, E**
Co	−6.2140	−7.4789 (H)	**S, E**
Ni	−5.2995	−5.2916 (B)	**S, E**
Cu	−3.072	−3.2239 (B)	NS
Zn	−0.6010	−0.9770 (B)	NS
Ge	−4.4386	−4.2877 (B)	NS
Sr	−1.2212	−1.2513 (H)	NS
Y	−4.5639	−2.8338 (H)	NS
Zr	−6.8608	−4.6825 (H)	**S, L**
Nb	−8.3449	−8.2461 (H)	**S, E**
Mo	−9.2626	−9.2706 (H)	**S, L**
Pd	−4.6656	−4.6930 (T)	**S, L**
Ag	−2.6550	−2.8060 (B)	NS
Cd	−0.5628	−0.9120 (B)	NS
In	−1.8208	−2.2433 (B)	NS
Sn	−3.3616	−3.5007 (B)	NS
Hf	−6.3668	−3.8109 (T)	**S, E**
Au	−3.8270	−4.0928 (B)	NS
Tl	−1.8947	−2.6318 (B)	NS
Pb	−2.8062	−3.2776 (B)	NS

between 0.0 and −1.0 eV, adsorbates are seen to obviously ascend above the surface, where from −1.0 to −2.0 eV a rather flat distribution of atoms is seen in the top layer, with the substitutional elements more or less preserving their initial positions. On the other hand, for surfaces with adsorption energies in between −2.0 and −6.0 eV, an apparent descent of the dopants is observed, where from −6.0 to −9.0 eV, there is a more obvious attraction of the elements inside the substrate as well as the slight distortion of surface atoms. It should certainly be taken into account that this is a somewhat general observation, with some exceptions present.

3.2. On-surface adsorption

Within the context of surface alloying studies, the other three positions for adatoms to be placed are hollow, top and bridge sites, as mentioned previously. Here, since the elements are located at a finite distance to the surface, adsorption of these species to the surface is named as on-surface or normal adsorption. In this respect, on-surface adsorption energies of each system, represented by $E_{nor\text{-}ads,Mg(0001)}$, were calculated via Eq. (2) for each of the three sites. The results were also given in Table 1, with initials of the lowest energy on-surface site indicated in parentheses. Normal mode analysis carried out in these systems, at which lowest adsorption energy was obtained, showed that the sites are indeed true minima with no imaginary frequencies. The calculated vibration frequencies of the alloying elements on top, bridge and hollow sites are in the range 27–174 cm^{-1}, 15–268 cm^{-1} and 29–178 cm^{-1}, respectively. The calculated adsorption energies again point out that, dopants in all systems would be normally adsorbed on magnesium substrate. Similar to the consequence arisen from substitutional adsorption, Mo, Nb, Mn, Co, Cr, Fe, V, P and Ni are among the adatoms with increased probabilities of adsorption, where energy values are in the range of −9.2706 (Mo) and −5.2916 eV (Ni). Cd, on the other hand, possesses the highest on-surface adsorption energy, which is −0.912 eV. Upon further examination of the results, it is seen that, for eighteen of the Mg surface structures, relatively lower adsorption energies are provided by bridge sites, for eleven of them by hollow sites, where only three of the systems are provided with lower values by top sites. Some inferences made from the final configurations are, besides the obvious or slight shifts of adatoms in the z direction, elements inserted in top positions generally seem to repulse the atom just underneath it towards the lattice, while itself is elevated in the vacuum to some extent. Another observation is about the Mn and Mo elements, that is, they lead to an apparent dispersion of top layer atoms.

3.3. MD simulations

Thirty four systems were studied for the surface molecular dynamics calculations of Mg. Principally, it was aimed to observe the dissociation and subsequent adsorption of hydrogen at the surface for each case. In other words, whether the substituted atoms exhibit an effect of catalyzer, in terms of the dissociation of hydrogen molecule into H atoms at the surface, or not. MD simulations were firstly executed on clean Mg (0001) surface (at the temperature in question, 300 K), within a limited simulation time. Even though the simulation continued for 10 ps, it was seen that the splitting of H_2 without any alloying addition is not possible, see Fig. 3, most probably due to the homogeneous charge distribution over the surface. Therefore, the need to dope some elements on magnesium surface in order to ease dissociation has become obvious. Simulation results (also indicated in Table 1) revealed that, systems alloyed with most of the transition metals are good at dissociating the hydrogen molecule.

The thirty four elements studied were grouped into two, as also indicated in Table 1, in terms of their success in splitting the hydrogen molecule. Those which were able to retain the H–H separation distance above 2–3 Å, once dissociation occurred, were classified as the splitting elements. The second class is the non-splitting characteristic, where H–H distance is maintained nearly at its equilibrium value which is less than 1 Å, during the entire simulation time. While some of the non-splitting elements have no effect on hydrogen action in vacuum, some are observed to repulse the hydrogen away from the surface to some extent, such as Cd, In and Zn. Although not studied extensively and not given in Table 1, the simulation executed for Mg surface-substituted with one oxygen atom supports the fact that hydrogen intake is inhibited by the oxygen presence at the surface [4], since H_2 is seen to be repelled away from the surface in this case. In summary, one can say that, 3*d* (from Ti to Ni) and 4*d* (from Zr to Pd) transition metals are accomplished in hydrogen dissociation.

A further categorization among the splitting dopants puts forth the rate of adsorption of one of the hydrogen atoms on the surface. According to this, we suggest the two groups as such: rapid (early) adsorption in between 30 and 200 fs and relatively slower (late) intake of hydrogen after 200–500 fs. In the early group, Mn, Fe, Co and Nb induce the fastest hydrogen adsorption on-surface within approximately 50 fs, while for systems doped with Cr, Ni and Hf it takes a little longer time for H to be attracted inside the slab of magnesium. For the transition metals other than the stated ones, which are Ti, V, Zr, Mo, Ru, Rh and Pd, hydrogen adsorption occurs within 250–500 fs.

Subsequently, outcome of the MD simulations were further analyzed by graphical means for each of the 34 systems mentioned

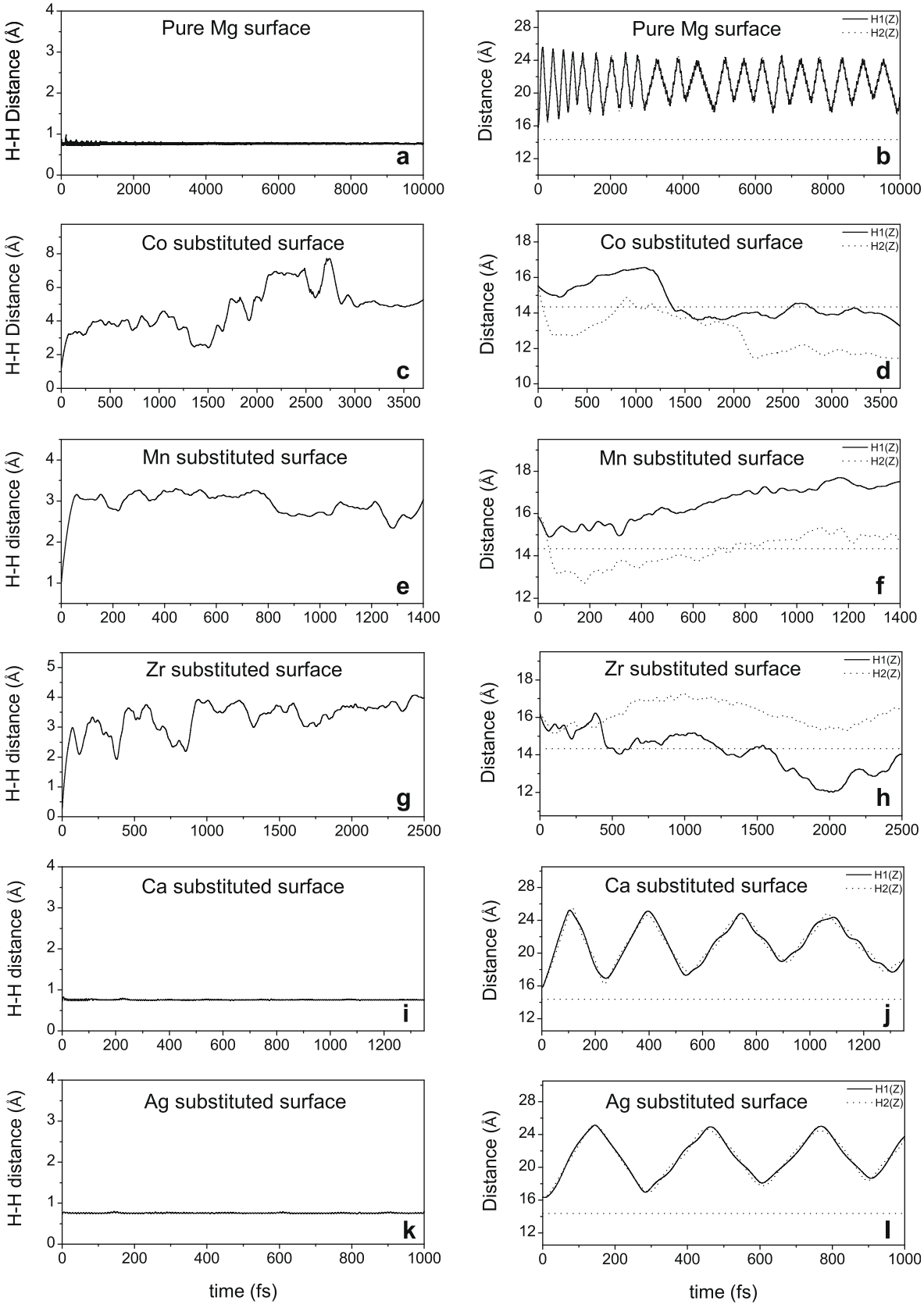

Fig. 3. The variation of separation between hydrogen atoms for (a) Pure Mg, (c) Co, (e) Mn, (g) Zr, (i) Ca and (k) Ag doped surfaces and the *z* coordinates of either hydrogen atom throughout the simulation for (b) Pure Mg, (d) Co, (f) Mn, (h) Zr, (j) Ca and (l) Ag substituted surface structures.

previously. In this respect, the distance between hydrogen atoms and positions of either hydrogen (H1 and H2) in *z* direction are given with respect to the simulation time in Fig. 3 for six representative systems, namely unalloyed, cobalt, manganese, zirconium,

calcium and silver doped magnesium surfaces. Fig. 3a shows clearly that the H_2 molecule is definitely not dissociated on pure magnesium surface, where in Fig. 3b H_2 is observed to be in a fluctuating motion within the vacuum region. On the other hand, as could be seen from Fig. 3c, the distance between H atoms reaches above 3 Å, immediately after 50 fs in Co substituted surface. From Fig. 3e, we observe that this takes approximately 30 fs for Mn substituted system. Fig. 3g displays that, for surface with Zr as an adsorbate, separation at around 3 Å takes place after 450 fs. Furthermore, Fig. 3i and k clearly exhibit the non-splitting behavior of H_2, where H atoms are never apart from each other during the simulation duration, preserving the molecule state. Moreover, as observable in Fig. 3d, f and h, right after the decomposition of H_2, one of the H's is being adsorbed on the surface and drawn into the slab (horizontal line represents the position of the surface). For Co substituted surface, the second hydrogen is also seen to be penetrated through the surface at around 1300 fs, as seen in Fig. 3d. From that point on, one of the hydrogen is attracted even more into the lattice where the other maintains its position around the surface. In the meantime, separation distance of H's is being kept above 3 Å. However, Fig. 3f and h display that, unlike the situation for Co, the second H atom does not proceed inside the adsorbent for Mn and Zr doped systems (as far as we can observe within the limited simulation time). As a final remark, by looking at Fig. 3j and l, we could state that both hydrogen atoms are oscillating above the surface, in molecule form. Finally, it is worth mentioning that, a separation of 3 Å could be considered as a criterion for full decomposition of the hydrogen molecule.

At first sight, each of the fourteen elements seems to achieve the catalyzer effect on H_2 dissociative adsorption. However, it is more pronounced specifically for the middle transition metals, whereas for the early and late transition metals the effect is somewhat delayed. Although middle transition metals generally have no or less stable binary hydrides [28,29], therefore less affinity to hydrogen, when alloyed on Mg surface they have a strong influence on H_2 dissociation.

Moreover, the correlation between molecular dynamics simulations and adsorption energy values of Mg $(0\,0\,0\,1)$ systems is of particular interest. The obvious relation between the two is that, dopants which have given satisfying results in MD calculations also contribute to the adsorption energies being more negative, or in other words, they hold relatively higher adsorption abilities on the surface.

3.4. Charge density difference plots

Charge density difference distributions on $(\bar{2}\,1\,1\,0)$ plane of Mg were computed for each system in order to depict the mechanism behind splitting of the hydrogen molecule, in terms of the effect of added elements. Firstly, the electron density distributions on relaxed M doped Mg surfaces were calculated individually as well as the distribution over pure Mg surface. Then, the difference between charge densities of the relaxed M doped structures and pure Mg surface having the same volume and atomic configuration were taken, so that it could be possible to take the difference point by point and investigate the charge dispersion around the adsorbates, from the dopant-effect point of view.

We assessed several characteristic behaviors of charge densities, as illustrated in Fig. 4, relying on the positions and grouping of the substituted elements in periodic table. According to this, an interesting behavior came out to be the spherical symmetry in accumulation of electrons around the adsorbed elements, which are Ag, Au, Cd, Cu, P, Tl and Zn. Another characteristic attribute is exhibited by Al, Ge, In, Pb, Si and Sn doped surfaces, where there is again a spherical denseness of electrons, however with lower charge values and a distorted spherical shape this time. Contrarily to the situations mentioned above, for alkaline metals such as Li, Na, K, Ca and Sr, charge depletion instead of accumulation is

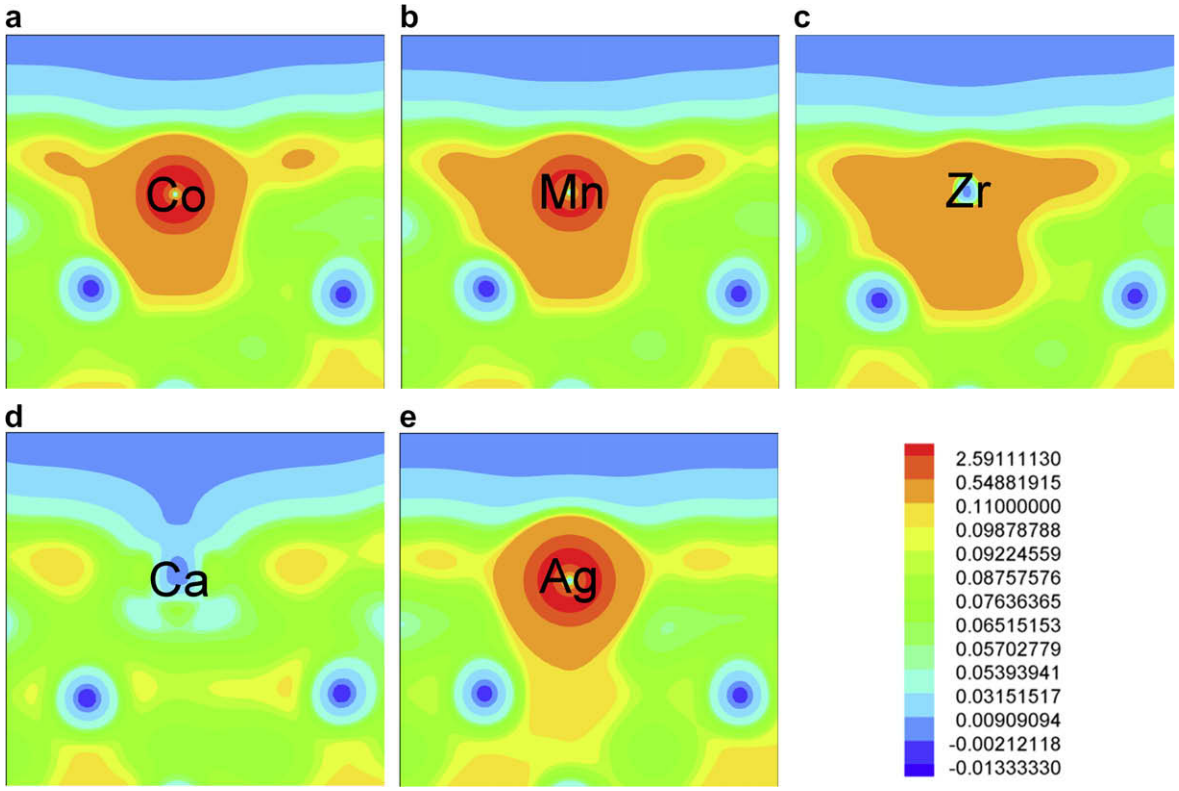

Fig. 4. Charge density difference distributions on $(\bar{2}\,1\,1\,0)$ crystal planes of the selected Mg surface structures alloyed with: (a) Co, (b) Mn, (c) Zr, (d) Ca and (e) Ag.

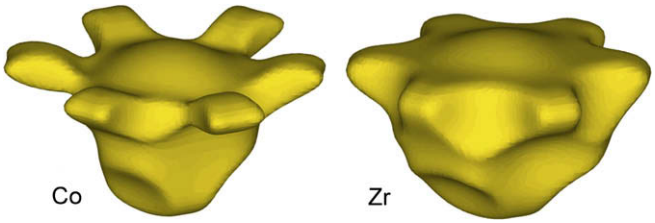

Fig. 5. Isosurfaces of charge density difference taken at the alloying element site for magnesium surface structures alloyed with Co and Zr elements, which were computed at 0.1 eu.

observed at the center site of magnesium–vacuum interface. Among these alkaline elements, Na exhibits the depletion effect most obviously. Moreover, K, Ca, Sr and Li also seem to have dispersed their charges to the surroundings.

Selective illustration of the charge density differences point out the common behaviors of hydrogen-dissociating elements (as shown in Fig. 4), which is the effective and oriented increase in electron density at the adsorbent–adsorbate interface. More specifically, elements such as Co, Cr, Fe, Mn and Ni display an important characteristic which is the upwards-oriented branches, aligned towards a direction in between the neighboring surface Mg atoms, in a six-fold like symmetry. The rapid dissociation of hydrogen molecule and immediate attraction of one of the hydrogen atoms inside the lattice could be attributed to this configuration, especially for Co, Fe and Mn elements. On the other hand, charge density difference plots for some of the late adsorbing surfaces are appealing, in terms of their rather spread and flat electron density distributions at the branches.

Fig. 4 presents samples from each of the characteristic groups, in the way that Co and Mn represent the fast adsorbing hydrogen splitting elements with the mentioned upwards-oriented branches in a six-fold like symmetry, pointing towards the neighboring Mg atoms (Fig. 4a and b). Furthermore, illustration regarding the Zr doped system (Fig. 4c) is a representative example of the late adsorbing splitting elements. The relatively dispersed and flat distribution of electronic density at the surface is obvious in this figure. On the other hand, Fig. 4d shows the obvious charge depletion around the adatom, which could be treated as an implication of the agreement in between the charge density difference plots and non-splitting characteristic of the alkaline elements. Finally, Ag stands as an example for the elements exhibiting nearly spherical symmetry around the dopant, which again points out the non-splitting behavior of several other elements.

A more detailed visualization of the upwards-oriented branches of the electronic density difference for fast adsorbing and flat distribution for late adsorbing surfaces is as displayed in Fig. 5, for example, for surfaces substituted with Co and Zr. These isosurfaces of charge density differences, taken at the alloying element site, clearly show the difference in the surface electronic state between the early and late hydrogen adsorbing surfaces, in terms of the characteristic H_2 dissociation behavior.

4. Conclusions

In summary, outcome of the adsorption energy calculations point out that, elements such as Mo, Nb, Mn, Cr, Co, Fe, V, P and Ni seem to possess higher probabilities of adsorption on the magnesium surface. Among the transition metals, there has been detected a trend in the way that, elements including and to the left of VIA column in the periodic table prefer to be adsorbed on substitutional sites (over hollow sites), while the transition elements to the right of VIA elements, generally have the tendency to be adsorbed on bridge sites.

MD simulations, on the other hand, gave us the chance to visualize which one of the selected thirty four elements would act as catalysts for the dissociation of hydrogen. Most of the transition metal elements (from Ti to Ni in 3*d* and from Zr to Pd in 4*d* series) were found to be beneficial dopants enabling the hydrogen dissociation and adsorption, due to their orbital occupancies. Especially, elements such as Co, Mn and Fe in 3*d* series are quite effective.

Charge density difference plots provided some ideas about why certain alloying elements on the surface enhance the adsorption of hydrogen. More specifically, especially for Co, Mn and Fe elements, a correspondence may be monitored between the outcome of electronic density distributions and MD simulations, which display the rapid dissociation of H_2 and immediate attraction of one of the H atoms.

A final remark could be on the correlation between the experimental results and theoretical calculations in this study, where in terms of catalysis, the power of 3*d* and even 4*d* transition metals, as emphasized several times [4–6,8,14,29,30] were verified. Although the slow adsorption/desorption kinetics of hydrogen still remains as a problem to be solved in practice, we hope that this study will guide some experimental approaches towards the effect of catalysis.

Acknowledgements

The authors gratefully acknowledge Turkish Scientific and Technical Research Council (TUBITAK) for financial support within the scientific research project 106M174. The numerical calculations reported in this paper were performed at the ULAKBIM High Performance Computing Center in TUBITAK, within the TR-Grid e-Infrastructure project.

References

[1] A. Züttel, Mater. Today 9 (2003) 24.
[2] L. Schlapbach, A. Züttel, Nature 414 (2001) 353.
[3] D.G. Ivey, D.O. Northwood, J. Mater. Sci. 18 (1983) 321.
[4] A. Zaluska, L. Zaluski, J.O. Ström–Olsen, J. Alloy Compd. 288 (1999) 217.
[5] R. Baer, Y. Zeiri, R. Kosloff, Phys. Rev. B 55 (1997) 10952.
[6] G. Liang, J. Huot, S. Boily, A. Van Neste, R. Schulz, J. Alloy Compd. 292 (1999) 247.
[7] W. Oelerich, T. Klassen, R. Bormann, J. Alloy Compd. 315 (2001) 237.
[8] M. Dornheim, S. Doppiu, G. Barkhordarian, U. Boesenberg, T. Klassen, O. Gutfleisch, R. Bormann, Scripta Mater. 56 (2007) 841.
[9] P.T. Sprunger, E.W. Plummer, Chem. Phys. Lett. 187 (1991) 559.
[10] D.M. Bird, L.J. Clarke, M.C. Payne, I. Stich, Chem. Phys. Lett. 212 (1993) 518.
[11] P. Ravindran, P. Vajeeston, R. Vidya, H. Fjellvåg, A. Kjekshus, J. Power Sources 159 (2006) 88.
[12] T. Vegge, Phys. Rev. B 70 (2004) 35412.
[13] T. Vegge, L.S. Hedegaard-Jensen, J. Bonde, T.R. Munter, J.K. Nørskov, J. Alloy Compd. 386 (2005) 1.
[14] M. Pozzo, D. Alfè, A. Amieiro, S. French, A. Pratt, J. Chem. Phys. 128 (2008) 94703.
[15] A. Kiejna, T. Ossowski, E. Wachowicz, Surf. Sci. 548 (2004) 22.
[16] G. Kresse, J. Hafner, Phys. Rev. B 47 (1993) 558; ibid. 49 (1994) 14251.
[17] G. Kresse, J. Furthmuller, Comput. Mater. Sci. 6 (1996) 15.
[18] G. Kresse, J. Furthmuller, Phys. Rev. B 54 (1996) 11169.
[19] J. Perdew, J. Chevary, S. Vosko, K. Jackson, M. Pederson, D. Singh, C. Fiolhais, Phys. Rev. B 46 (1992) 6671.
[20] D. Vanderbilt, Phys. Rev. B 41 (1990) 7892.
[21] J. Neugebauer, M. Scheffler, Phys. Rev. B 46 (1992) 16067.
[22] K. Momma, F. Izumi, J. Appl. Crystallogr. 41 (2008) 653.
[23] S. Nosé, J. Chem. Phys. 81 (1984) 511.
[24] S. Nosé, Mol. Phys. 52 (1984) 255.
[25] P. Villars, Pearson's Handbook: Crystallographic Data for Intermetallic Phases, ASM International Desk Edition (1997).
[26] B. Bogdanovic, K. Bohmhammel, B. Christ, A. Reiser, K. Schlichte, R. Vehlen, U. Wolf, J. Alloy Compd. 282 (1999) 84.
[27] Y. Song, Z.X. Guo, R. Yang, Phys. Rev. B 69 (2004) 94205.
[28] H. Smithson, C.A. Marianetti, D. Morgan, A. Van der Ven, A. Predith, G. Ceder, Phys. Rev. B 66 (2002) 144107.
[29] K.H.J. Buschow, P.C.P. Bouten, A.R. Miedema, Rep. Prog. Phys. 45 (1982) 937.
[30] B. Sakintuna, F. Lamari-Darkrim, M. Hirscher, Int. J. Hydrogen Energy 32 (2007) 1121.